CHALMERS

FINITE ELEMENT CENTER

PREPRINT 2002-12

Discontinuous Least-Squares Finite Element Methods for the Div-Curl Problem

Rickard Bergström and Mats G. Larson

Chalmers Finite Element Center
CHALMERS UNIVERSITY OF TECHNOLOGY
Göteborg Sweden 2002

CHALMERS FINITE ELEMENT CENTER

Preprint 2002-12

Discontinuous Least-Squares Finite Element Methods for the Div-Curl Problem

Rickard Bergström and Mats G. Larson

CHALMERS

Chalmers Finite Element Center
Chalmers University of Technology
SE–412 96 Göteborg Sweden
Göteborg, December 2002

Discontinuous Least-Squares Finite Element Methods for the Div-Curl Problem
Rickard Bergström and Mats G. Larson
NO 2002-12
ISSN 1404–4382

Chalmers Finite Element Center
Chalmers University of Technology
SE–412 96 Göteborg
Sweden
Telephone: +46 (0)31 772 1000
Fax: +46 (0)31 772 3595
www.phi.chalmers.se

Printed in Sweden
Chalmers University of Technology
Göteborg, Sweden 2002

Discontinuous Least-Squares Finite Element Methods for the Div-Curl Problem *

Rickard Bergström† and Mats G. Larson‡

Abstract

In this paper, we consider the div-curl problem posed on nonconvex polyhedral domains. We propose a least-squares method based on discontinuous elements with normal and tangential continuity across interior faces, as well as boundary conditions, weakly enforced through a properly designed least-squares functional. Discontinuous elements make it possible to take advantage of regularity of given data (divergence and curl of the solution) and obtain convergence also on nonconvex domains. In general, this is not possible in the least-squares method with standard continuous elements. We show that our method is stable, derive a priori error estimates, and present numerical examples illustrating the method.

1 Introduction

The least squares finite element method is a general technique for finding the approximate solution of first order partial differential equations based on minimization of the L^2-norm of the residual over a suitable finite element space. Second order problems are first written as first order systems by introducing additional, often physically motivated, variables. The method manufactures symmetric positive definite algebraic systems which are suitable for applying iterative techniques to find the solution, for instance multigrid. For an overview of least-squares finite element methods, we refer to [7] and the references therein.

In this paper, we develop a least-squares method for the div-curl problem posed on a nonconvex polyhedral domain with discontinuous piecewise constant coefficients and a right hand side, defined on a partition of the domain into (possibly nonconvex) subdomains, which is piecewise sufficiently smooth ($H^\alpha, \alpha \geq 0$). This problem serves as an important model problem in electromagnetics and also arises when a curl-term is added as stabilization when solving the second order elliptic problem, see, e.g., [10] and [21].

*Research supported by ABB Corporate Research, Sweden

†Supported by the Swedish Foundation for Strategic Research through the National Graduate School in Scientific Computing and the National Network in Applied Mathematics

‡Supported by Swedish Research Council for Engineering Sciences

Standard least-squares finite element methods typically require rather strong regularity on the exact solution. For instance, in most works a convex domain is required. This problem has been studied and at least two different solution approaches have been presented, both based on weaker measurements of the residual. The first uses a weighted norm with a radial weight in the vicinity of corners, see Cox and Fix [13] and Manteuffel *et al.* [19]. The second approach is to replace the L^2-norm by a discrete approximation of the H^{-1}-norm, see Bramble *et al.* [9]. Both these methods are somewhat complicated to implement; the first requires knowledge of a local weight of suitable strength at each corner or line singularity and in the second, an implementation of the discrete version of the H^{-1}-norm is needed.

Instead, we propose using discontinuous approximation spaces where tangential and normal continuity, as well as boundary conditions, are weakly enforced through a properly defined least-squares functional. Such spaces make it possible to take advantage of the regularity of the given right hand side and obtain convergence also in the nonconvex case. For efficiency reasons we formulate a hybrid scheme, where discontinuous elements only are employed in the vicinity of corners where it is necessary. Away from the singularities, the solution is regular and continuous, typically higher order, polynomials may be used.

In the analysis we consider the simplified case when the coefficient equals the identity, and comment on the extension to space varying data. We prove coercivity with respect to the H(div,curl)-norm and a priori error estimates of optimal order.

We also present numerical results for model problems in three spatial dimensions. The problems include a line singularity, a point singularity and a magnetostatic interface problem, where the coefficient exhibits a large jump across the interface.

The paper is organized as follows. In Section 2, we present the div-curl problem and the least-squares method; in Section 3, we prove coercivity of the bilinear form with respect to the H(div, curl)-norm for simplified model problems and a priori error estimates; in Section 4, we introduce a hybrid formulation suitable for efficient computations together with the natural mesh refinement indicator; in Section 5, we present numerical results.

2 The least-squares finite element method

2.1 Model problem

We consider the problem: find $u : \Omega \to \mathbf{R}^3$ such that

$$\nabla \times Au = \omega \quad \text{in } \Omega, \tag{2.1a}$$

$$\nabla \cdot u = \rho \quad \text{in } \Omega, \tag{2.1b}$$

$$n \times Au = 0 \quad \text{on } \Gamma_T, \tag{2.1c}$$

$$n \cdot u = 0 \quad \text{on } \Gamma_N, \tag{2.1d}$$

where $\Omega \subset \mathbf{R}^3$ is a polyhedral domain with boundary $\Gamma = \Gamma_T \cup \Gamma_N$, see Grisvard [16] for a definition. By subscripts T and N we refer to the tangential and normal traces, ω

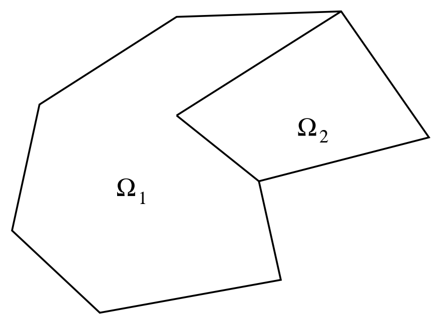

Figure 1: A polygonal domain with two subdomains.

and $\rho \in [L^2(\Omega)]^3$ are given functions, n is the exterior unit normal to Γ, A is a piecewise constant function $A = A^i$ for $x \in \Omega^i$, with $\{\Omega^i\}$ a partition of Ω into polyhedral subdomains Ω^i.

Natural spaces for this problem are

$$H(\mathrm{div};\Omega) = \{v \in [L^2(\Omega)]^3 : \nabla \cdot v \in L^2(\Omega)\}, \tag{2.2a}$$
$$H(\mathrm{curl}A;\Omega) = \{v \in [L^2(\Omega)]^3 : \nabla \times Av \in [L^2(\Omega)]^3\}, \tag{2.2b}$$
$$H(\mathrm{div},\mathrm{curl}A;\Omega) = H(\mathrm{div};\Omega) \cap H(\mathrm{curl}A;\Omega), \tag{2.2c}$$

which are Sobolev spaces with their respective product norms,

$$\|v\|^2_{H(\mathrm{div})} = \|\nabla \cdot v\|^2 + \|v\|^2, \tag{2.3a}$$
$$\|v\|^2_{H(\mathrm{curl})} = \|\nabla \times v\|^2 + \|v\|^2, \tag{2.3b}$$
$$\|v\|^2_{H(\mathrm{div},\mathrm{curl})} = \|\nabla \cdot v\|^2 + \|\nabla \times v\|^2 + \|v\|^2. \tag{2.3c}$$

Under our assumptions on data, the solution u to (2.1) resides in at least $[H^{1/2}(\Omega)]^3$, since the subspace of $H(\mathrm{div},\mathrm{curl};\Omega)$ restricted to functions with traces that fulfil (2.1c)-(2.1d), are embedded in $[H^s(\Omega)]^3$, with $s > 1/2$, see [1] and [12]. For convex domains, we have $s = 1$.

2.2 Finite element spaces

Let $\mathcal{K}$ be a triangulation of Ω into shape regular tetrahedra K which respects the subdomains, i.e., all $K \subset \Omega^i$ for some i. Denote the set of all faces F by $\mathcal{F}$ and divide $\mathcal{F}$ into three disjoint sets,

$$\mathcal{F} = \mathcal{F}_I \cup \mathcal{F}_T \cup \mathcal{F}_N, \tag{2.4}$$

where $\mathcal{F}_I$ is the set of all faces in the interior of Ω, $\mathcal{F}_T$ the faces on Γ_T, and $\mathcal{F}_N$ the faces on Γ_N. We let $h : \Omega \to \mathbf{R}$ denote the mesh function such that $h|_K = h_K = \mathrm{diam}(K)$

and $h|_F = h_F = \text{diam}(F)$, i.e., a measure of the size of the face F. Finally, we define the discontinuous piecewise polynomial space

$$\mathcal{V}_h = [\mathcal{DP}_p]^3, \tag{2.5}$$

where

$$\mathcal{DP}_p = \bigoplus_{K \in \mathcal{K}} \mathcal{P}_p(K), \tag{2.6}$$

and $\mathcal{P}_p(K)$ is the space of all polynomials of degree less than or equal to p defined on K. The degree of the polynomials, as well as the meshsize, may vary from element to element so that $p|_K = p_K$, thus allowing h-p adaptivity.

2.3 The discontinuous least-squares finite element method

DLSFEM, the discontinuous least-squares finite element method, reads: find $u_h \in \mathcal{V}_h$ such that

$$I(u_h) = \inf_{v \in \mathcal{V}_h} I(v), \tag{2.7}$$

where the least-squares functional $I(\cdot)$ is defined by

$$\begin{aligned} I(v) = &\sum_{K \in \mathcal{K}} \Big(\|A^{-1/2}(\nabla \times Av - \omega)\|_K^2 + \|A^{1/2}(\nabla \cdot v - \rho)\|_K^2 \Big) \\ &+ \sum_{F \in \mathcal{F}_I \cup \mathcal{F}_T} \Big(\|h^{1/2} A_T^{-1/2} Q_0 [n \times Av]\|_F^2 + \|h^{-1/2} A_T^{1/2} P_0 [n \times v]\|_F^2 \Big) \\ &+ \sum_{F \in \mathcal{F}_I \cup \mathcal{F}_N} \Big(\|h^{1/2} A_N^{1/2} Q_0 [n \cdot v]\|_F^2 + \|h^{-1/2} A_N^{1/2} P_0 [n \cdot v]\|_F^2 \Big). \end{aligned} \tag{2.8}$$

Here we used the following notation: P_0 is the L^2-projection on constant functions on each face F and $Q_0 = I - P_0$ with I the identity operator; n is a fixed unit normal to $F \in \mathcal{F}_I$ and the exterior unit normal for $F \in \mathcal{F}_T \cup \mathcal{F}_N$; $[v] = v^+ - v^-$ for $F \in \mathcal{F}_I$ and $[v] = v^+$ for $F \in \mathcal{F}_T \cup \mathcal{F}_N$, where $v^\pm(x) = \lim_{s \to 0, s > 0} v(x \mp sn)$ for $x \in F$; $A_N = 2A^+A^-/(A^+ + A^-)$ and $A_T = (A^+ + A^-)/2$. Note that both differential equations (2.1a) and (2.1b) and boundary conditions (2.1c) and (2.1d), as well as tangential and normal continuity on interior faces, are imposed weakly through the least-squares functional.

Remark 2.1 We may use weighting of the different terms in the least-squares functional by inserting a positive constant in front of each term, see [11]. Weighting leads to a different, but equivalent, discrete approximation. To simplify the notation, we have not included these weights.

The corresponding variational equation takes the form: find $u_h \in \mathcal{V}_h$ such that

$$a(u_h, v) = l(v), \tag{2.9}$$

for all $v \in \mathcal{V}_h$. Here $a(\cdot,\cdot)$ is a bilinear form and $l(\cdot)$ a linear functional, defined by

$$\begin{aligned} a(u,v) = \sum_{K\in\mathcal{K}} (A^{-1}\nabla\times Au, \nabla\times Av)_K + (A\nabla\cdot u, \nabla\cdot v)_K \quad (2.10a) \\ + \sum_{F\in\mathcal{F}_I\cup\mathcal{F}_T} \big((hA_T^{-1}Q_0[n\times Au], Q_0[n\times Av])_F \\ + (h^{-1}A_T^{-1}P_0[n\times Au], P_0[n\times Av])_F\big) \\ + \sum_{F\in\mathcal{F}_I\cup\mathcal{F}_N} \big((hA_N Q_0[n\cdot u], Q_0[n\cdot v])_F \\ + (h^{-1}A_N P_0[n\cdot u], P_0[n\cdot v])_F\big), \end{aligned}$$

$$l(v) = \sum_{K\in\mathcal{K}} (A^{-1}\omega, \nabla\times Av)_K + (A\rho, \nabla\cdot v)_K. \quad (2.10b)$$

3 Error estimates

Throughout this section, we assume that $A = I$, with I the identity matrix, Ω is a nonconvex polyhedral domain, and $\Gamma = \Gamma_N$. Based on the decompositions by Bonnet-Ben Dhia *et al.*[8], our analysis can directly be extended to the case $\Gamma = \Gamma_T$ and, with sufficiently smooth interface boundaries, $A \neq I$. These assumptions are necessary to prove the coercivity of Theorem 3.1, while the error estimate in the least-squares norm in Theorem 3.5 holds for the general problem (2.1).

3.1 The least-squares norm

We define the natural least-squares norm, or energy norm,

$$|||v|||^2 = a(v,v), \quad (3.1)$$

for all $v \in \mathcal{V}_h + H(\text{div}, \text{curl}; \Omega) \cap H^{1/2}(\Omega)$. We then have the following result which shows that $|||\cdot|||$ is indeed a norm on this space.

Theorem 3.1 *There is a constant C, independent of h, such that*

$$\|v\| \le C|||v|||, \quad (3.2)$$

for all $v \in \mathcal{V}_h + H(div, curl; \Omega) \cap H^{1/2}(\Omega)$.

In order to prove this estimate we first establish a suitable Helmholtz decomposition of $[L^2(\Omega)]^3$.

Lemma 3.2 *For each $v \in [L^2(\Omega)]^3$ there is $\chi \in [H^1]^3(\Omega)$ and $\phi \in H^1(\Omega)$ such that*

$$v = \nabla\times\chi + \nabla\phi. \quad (3.3)$$

Furthermore, the stability estimates

$$\|\chi\|_1 \leq C\|v\|, \tag{3.4a}$$

$$\|\phi\|_1 \leq C\|v\|, \tag{3.4b}$$

hold.

Proof. Let ϕ be the solution of the Neumann problem: find $\phi \in H^1(\Omega)$ such that

$$(\nabla\phi, \nabla w) = -(\nabla \cdot v, w) + (n \cdot v, w)_\Gamma, \tag{3.5}$$

for all $w \in H^1(\Omega)$. Then $\nabla \cdot (v - \nabla\phi) = 0$ and $n \cdot (v - \nabla\phi) = 0$ on Γ. Thus there exists $\chi_0 \in H(\text{curl};\Omega)$ such that $\nabla \times \chi_0 = v - \nabla\phi$ and $n \times \chi_0 = 0$ on Γ [15]. Note that the boundary condition $n \times \chi_0 = 0$ implies $n \cdot \nabla \times \chi_0 = n \cdot (v - \nabla\phi) = 0$.

Using Lemma 2.1 in Pasciak and Zhao [20] there exists $\chi \in [H^1(\Omega)]^3$ with $n \times \chi = 0$ on Γ and $\nabla \times \chi = \nabla \times \chi_0$. Furthermore, the stability estimate

$$\|\chi\|_1 \leq C\|\nabla \times \chi_0\|, \tag{3.6}$$

holds.

The decomposition (3.3) is thus established. Finally, we note that

$$\|v\|^2 = \|\nabla \times \chi_0\|^2 + \|\nabla\phi\|^2. \tag{3.7}$$

Then (3.4b) follows immediately and (3.4a) follows by using (3.6). □

Proof of Theorem 3.1. Using Lemma 3.2, we write

$$v = \nabla \times \chi + \nabla\phi. \tag{3.8}$$

Multiplying with v, integrating, and using integration by parts, gives

$$\|v\|^2 = \sum_{K\in\mathcal{K}} (v, \nabla \times \chi)_K + (v, \nabla\phi)_K \tag{3.9}$$

$$= \sum_{K\in\mathcal{K}} (\nabla \times v, \chi)_K - (\nabla \cdot v, \phi)_K \tag{3.10}$$

$$+ \sum_{F\in\mathcal{F}_I} ([n \times v], \chi)_F + \sum_{F\in\mathcal{F}} ([n \cdot v], \phi)_F.$$

Using the Cauchy-Schwarz inequality, definition of the $|||\cdot|||$-norm , and stability estimates (3.4), we get

$$\sum_{K\in\mathcal{K}} (\nabla \times v, \chi)_K \leq \sum_{K\in\mathcal{K}} \|\nabla \times v\|_K \|\chi\|_K \leq C|||v|||\,\|v\|, \tag{3.11}$$

$$\sum_{K\in\mathcal{K}} (\nabla \cdot v, \phi)_K \leq \sum_{K\in\mathcal{K}} \|\nabla \cdot v\|_K \|\phi\|_K \leq C|||v|||\,\|v\|. \tag{3.12}$$

Next we turn to the edge terms. Writing $v = Q_0 v + P_0 v$, we have

$$|([n \times v], \chi)_F| \leq \|h^{1/2}[n \times Q_0 v]\|_F h_K^{-1/2} \|Q_0 \chi\|_F \\ + \|h^{-1/2}[n \times P_0 v]\|_F h_K^{1/2} \|\chi\|_F. \tag{3.13}$$

We recall the trace inequality $\|w\|_F \leq C(h_K^{-1/2}\|w\|_K + h_K^{1/2}\|\nabla w\|_K)$, with F a face on ∂K. To estimate $\|Q_0\chi\|_F$, we first write $Q_0\chi = (I - P_0)\chi$ on F and then use the trace inequality

$$h_K^{-1/2}\|Q_0\chi\|_F \leq C h_K^{-1/2}\big(h_K^{-1/2}\|\chi - P_{0,K}\chi\|_K \\ + h_K^{1/2}\|\nabla(\chi - P_{0,K}\chi)\|_K\big) \tag{3.14}$$

$$\leq C\|\nabla\chi\|_K, \tag{3.15}$$

where $P_{0,K}$ is the $L^2(K)$ projection on $\mathcal{P}_0(K)$ and we applied the standard estimate $\|\chi - P_{0,K}\chi\|_K \leq C h_K \|\nabla\chi\|$.

Next we have

$$h_K^{1/2}\|\chi\|_F \leq C h_K^{1/2}\big(h_K^{-1/2}\|\chi\|_K + h_K^{1/2}\|\nabla\chi\|_K^2\big) \tag{3.16}$$

$$\leq C\|\chi\|_{1,K}. \tag{3.17}$$

Collecting these estimates and using stability estimate (3.4a), we arrive at

$$|([n \times v], \chi)_F| \leq C|||v|||\,\|v\| \tag{3.18}$$

The remaining boundary term is estimated in the same way. Finally, dividing by $\|v\|$, the desired estimate follows. □

3.2 Interpolation error estimates

We begin by introducing the interpolation operator $\pi : H(\mathrm{div}, \mathrm{curl}; \Omega) \cap [H^{1/2}(\Omega)]^3 \to \mathcal{V}_h$, such that $\pi u|_K = \pi_K u$ where $\pi_K : H(\mathrm{div}, \mathrm{curl}; K) \cap [H^{1/2}(K)]^3 \to [\mathcal{P}_1(K)]^3$ is defined by

$$\int_F u \cdot v \; dS = \int_F \pi_K u \cdot v \; dS, \tag{3.19}$$

for each face $F \subset \partial K$ and all $v \in [\mathcal{P}_0(F)]^3$. From this definition we derive the following two identities

$$\nabla \times \pi_K u = P_{0,K} \nabla \times u, \tag{3.20a}$$

$$\nabla \cdot \pi_K u = P_{0,K} \nabla \cdot u, \tag{3.20b}$$

where $P_{0,K}$ is the $L^2(K)$-projection on $[\mathcal{P}_0(K)]^3$. For instance, we have

$$\int_K \nabla \times (u - \pi_K u) \cdot v \; dx = \int_{\partial K} n \times (u - \pi_K u) \cdot v \; dS = 0, \tag{3.21}$$

for all $v \in [\mathcal{P}_0(K)]^3$. Using (3.20), we arrive at

$$\nabla \times u - \nabla \times \pi_K u = (I - P_{0,K})\nabla \times u. \tag{3.22}$$

Applying standard estimates for the L^2-projection, we can deduce the following lemma.

Lemma 3.3 *Let K be an affine element. Then there is a constant C depending only on the shape of K, such that*

$$\|\nabla \times (u - \pi u)\|_K \leq C h_K^\beta |\nabla \times u|_{\beta,K}, \tag{3.23}$$

$$\|\nabla \cdot (u - \pi u)\|_K \leq C h_K^\beta |\nabla \cdot u|_{\beta,K}, \tag{3.24}$$

with $0 \leq \beta \leq 1$.

We then have the following interpolation error estimate.

Lemma 3.4 *For $u \in [H^\alpha(\Omega)]^3$, $\alpha \geq 1/2$, with $\nabla \times u \in [H^\beta(\Omega)]^3$ and $\nabla \cdot u \in H^\beta(\Omega)$, $\beta \geq 0$, it holds*

$$|||u - \pi u|||^2 \leq C \sum_{K \in \mathcal{K}} h_K^{2\alpha} \|u\|_{\alpha,K}^2 + h_K^{2\beta}\big(\|\nabla \times u\|_{\beta,K}^2 + \|\nabla \cdot u\|_{\beta,K}^2\big), \tag{3.25}$$

with the constant C independent of h.

Proof. Using the interpolation error estimates in Lemma 3.3, we get

$$\|\nabla \times (u - \pi u)\|_K \leq C h_K^\beta \|\nabla \times u\|_{K,\beta}, \tag{3.26}$$

$$\|\nabla \cdot (u - \pi u)\|_K \leq C h_K^\beta \|\nabla \cdot u\|_{K,\beta}. \tag{3.27}$$

We now turn to the face contributions. Using the triangle inequality we have

$$\|Q_0[n \times (u - \pi u)]\|_F \leq \|Q_0 n \times (u - \pi u^+)\|_F + \|Q_0 n \times (u - \pi u^-)\|_F, \tag{3.28}$$

where face $F = \bar{K^+} \cap \bar{K^-}$ is shared by elements K^+ and K^-, and $\pi u^\pm = \pi u|_{K^\pm}$. Each term on the right hand side of (3.28) can now be estimated as

$$\begin{aligned} h_F\|Q_0 n \times (u - \pi u)\|_F^2 + h_F\|Q_0 n \cdot (u - \pi u)\|_F^2 &= h_F\|Q_0(u - \pi u)\|_F^2 \\ &\leq C h_F \|u - \pi u\|_{K,1/2}^2 \leq C h_K^{2\alpha}\|u\|_{K,\alpha}^2, \end{aligned} \tag{3.29}$$

with $\alpha \geq 1/2$, $K = K^\pm$, and $\pi u = \pi u^\pm$. For the second face contribution we have the identity

$$h_F^{-1}\|P_0 n \times (u - \pi u)\|_F^2 + h_F^{-1}\|P_0 n \cdot (u - \pi u)\|_F^2 = h_F^{-1}\|P_0(u - \pi u)\|_F^2 = 0, \tag{3.30}$$

where we used the definition of the interpolant in the last equality. □

3.3 A priori error estimate

Now, we are ready to state the following main result:

Theorem 3.5 *Let $u \in [H^\alpha(\Omega)]^3$, $\alpha \geq 1/2$, with $\nabla \times u \in [H^\beta(\Omega)]^3$ and $\nabla \cdot u \in H^\beta(\Omega)$, $\beta \geq 0$, be the exact solution to (2.1) and $u_h \in \mathcal{V}_h$ the approximate solution defined by (2.9). Then it holds*

$$|||u - u_h|||^2 \leq C \sum_{K \in \mathcal{K}} h_K^{2\alpha} \|u\|_{\alpha,K}^2 + h_K^{2\beta} \big(\|\nabla \times u\|_{\beta,K}^2 + \|\nabla \cdot u\|_{\beta,K}^2 \big), \tag{3.31}$$

with constant C independent of the meshsize h.

Proof. By the definition of the least squares method we have

$$|||u - u_h||| \leq |||u - \pi u|||, \tag{3.32}$$

and thus estimate (3.31) follows immediately from the interpolation error estimate. □
Combining Theorems 3.1 and 3.5 we get the following corollary.

Corollary 3.1 *Under the same assumptions as in Theorem 3.5 it holds*

$$\sum_{K \in \mathcal{K}} \|u - u_h\|_{H(K,div,curl)}^2 \leq C \sum_{K \in \mathcal{K}} h_K^{2\alpha} \|u\|_{\alpha,K}^2 + h_K^{2\beta} \big(\|\nabla \times u\|_{\beta,K}^2 + \|\nabla \cdot u\|_{\beta,K}^2 \big). \tag{3.33}$$

4 A hybrid formulation

Since the solution is of low regularity only close to the singularities, it is natural to use the computationally expensive discontinuous elements only in this region and use continuous elements in the smooth region. Denote by Ω_D a region, conforming with the triangulation $\mathcal{K}$, surrounding the geometric singularities, where we have to use DLSFEM, and let $\Omega_C = \Omega \backslash \Omega_D$. In Ω_C we have the solution $u \in [H^{s_C}]^3$, with $s_C \geq 1$, and may use continuous LSFEM, with polynomials of degree p_C. If the decomposition $\Omega = \Omega_C \cup \Omega_D$ is chosen such that s_C is considerably larger than s, we can also benefit from this by using high order polynomials in Ω_C. Further, let $\mathcal{K}_D = \{K \in \mathcal{K} : K \subset \Omega_D\}$ be the elements covering Ω_D, and define $\mathcal{K}_C$ analogously. An interpolation operator of Scott-Zhang type [22] is used for the continuous approximation.

We then have the following extension of our earlier a priori error estimate:

Corollary 4.1 *Under the same assumptions as in Theorem 3.5 it holds*

$$\begin{aligned} \sum_{K \in \mathcal{K}} \|u - u_h\|_{H(div,curl,K)}^2 \leq & \; C \sum_{K \in \mathcal{K}_D} h_K^{2\alpha} \|u\|_{\alpha,K}^2 + h_K^{2\beta} \big(\|\nabla \times u\|_{\beta,K}^2 + \|\nabla \cdot u\|_{\beta,K}^2 \big) \\ & + C \sum_{K \in \mathcal{K}_C} h_K^{2\alpha_C} \|u\|_{\alpha_C+1,K}^2. \end{aligned} \tag{4.1}$$

with $\alpha_C = \min(p_C + 1, s_C)$.

5 Numerical examples

We present in this section examples in domains in three spatial dimensions having corners, or subdomains with corners. We use the least-squares functional as mesh refinement indicator, since it exactly represents the error measured in energy norm $|||\cdot|||$ [18]. Moreover, we use an isotropic mesh refinement algorithm, splitting each element marked for refinement into two to eight new elements by successively dividing the longest edge, see [6] for more details. For these singular problem, it is however clear that we would gain from using an anisotropic error estimator and mesh refinement, see for instance [2], [14], and [23].

5.1 First order Poisson system

Here we consider the Poisson system: find p such that

$$-\Delta p = f \quad \text{in } \Omega, \tag{5.1a}$$
$$n \cdot \nabla p = g_N \quad \text{on } \Gamma_N, \tag{5.1b}$$
$$p = g_D \quad \text{on } \Gamma_D. \tag{5.1c}$$

Introducing the flux

$$u = \nabla p, \tag{5.2}$$

we may write problem (5.1) as a first order system: find (p, u) such that

$$-\nabla \cdot u = f \quad \text{in } \Omega, \tag{5.3a}$$
$$u - \nabla p = 0 \quad \text{in } \Omega, \tag{5.3b}$$
$$\nabla \times u = 0 \quad \text{in } \Omega, \tag{5.3c}$$
$$n \cdot u = g_N \quad \text{on } \Gamma_N, \tag{5.3d}$$
$$n \times u = n \times \nabla g_D \quad \text{on } \Gamma_D, \tag{5.3e}$$
$$p = g_D \quad \text{on } \Gamma_D. \tag{5.3f}$$

The curl-constraint (5.3c) is added since we then, on a convex domain, achieve H^1-coercivity for the system [10]. It arises from equation (5.2) and the fact that the curl of a gradient is identically zero.

We note that (5.3a), (5.3c), (5.3d), and (5.3e) completely define u, which thus can be solved independently of p in a first step. The latter is computed in a second step, by solving (5.3b) and (5.3f) with u as data.

We have applied the method described in this paper to solve the div-curl system of the first step on two problems posed on nonconvex domains, and then computed p by standard LSFEM [19].

5.1.1 Line singularity

We solve problem (5.3) and Ω the L-shaped domain displayed in Figure 2 with $z \in (0, 0.2)$, $\Gamma_N = \{x \in \Omega; z = 0.0 \text{ or } z = 0.2\}$ and $\Gamma_D = \partial\Omega \backslash \Gamma_N$, $f = 0$, and g_D chosen so that the

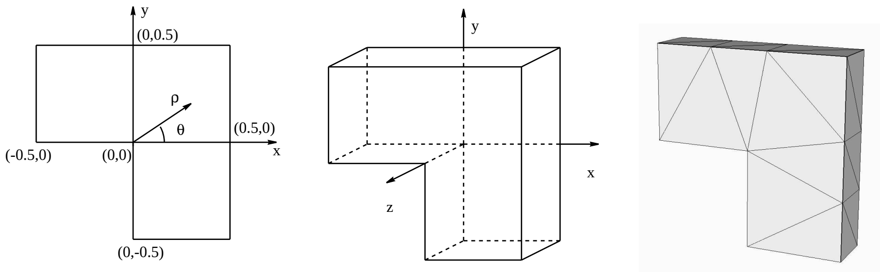

(a) *The x-y plane* (b) *The domain* (c) *Initial mesh*

Figure 2: The L-shaped domain with a line singularity.

exact solution p is

$$p(\rho, \theta, z) = \rho^{2/3} \sin(2\theta/3 + \pi/3). \tag{5.4}$$

The error, measured in $H^1(\Omega) \times H(\mathrm{div}, \mathrm{curl}; \Omega)$-norm, is plotted in Figure 3. In this figure, also the least-squares functional is plotted. We note that the behaviour of our modified method is the same as reported in [5] when the stabilizing curl-term was not included. The convergence of the algebraic solver is however much better when considering this compatibility constraint. In Figure 4(b) we can see the solution in the corner, displaying correctly the singularity and with the flux orthogonal to the boundary. On the contrary, standard LSFEM does not work in this setting. Instead we note that, in order to satisfy the conflicting constraints, the flux tends to zero in the corner, see Figure 4(a).

5.1.2 Point singularity

In this section, the domain where we solve (5.3) is $\Omega = \{(r, \theta, \phi) : r \in [0, 1), \theta \in (\beta, \pi], \phi \in [0, 2\pi)\}$ with $\beta = \pi/16$, described in spherical coordinates.

Also here $f = 0$, and we choose $g_D = P_\nu$, where P_ν is the first class Legendre function of order ν, and $\Gamma_D = \partial\Omega$. The exact solution p to this problem is

$$p(r, \theta) = r^\nu P_\nu(\cos(\theta)), \tag{5.5}$$

with ν depending on β; in our case we have $\nu \simeq 0.215$ for $\beta = \pi/16$, see [17]. A plot of the error is shown in Figure 6. The behaviour is similar as for the previous case, and also here the use of continuous elements fails.

5.2 The magnetostatic equations

The equations that define static magnetic fields are

$$\nabla \times H = J, \tag{5.6a}$$
$$\nabla \cdot B = 0, \tag{5.6b}$$

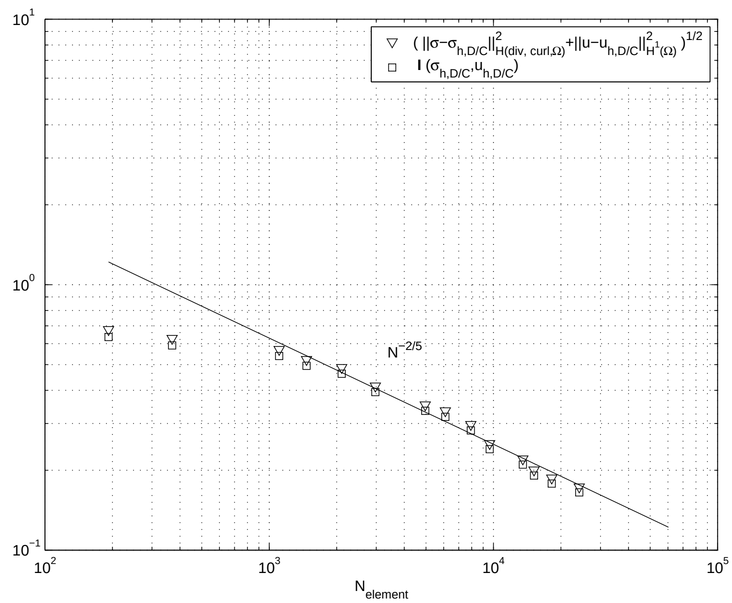

Figure 3: Error for DLSFEM in the line singularity problem. Triangles denote the error measured in the $H^1(\Omega) \times H(\text{div}, \text{curl}; \Omega)$-norm and squares denote the least-squares residual.

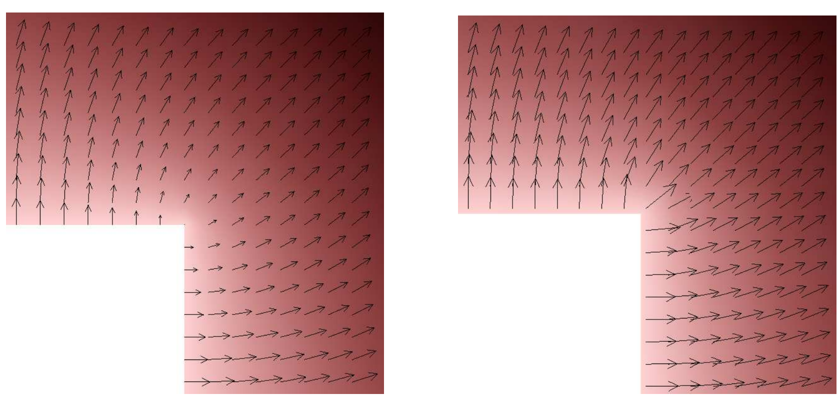

(a) *Standard LSFEM* (b) *Discontinuous LSFEM*

Figure 4: The computed flux in the vicinity of the corner of the L-shaped domain. Note that for standard LSFEM, the flux incorrectly tends to zero in the corner.

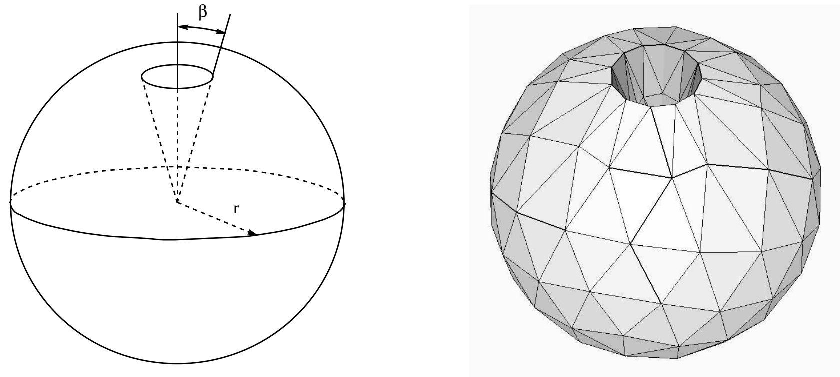

(a) *Geometry* (b) *Initial mesh*

Figure 5: The cone problem with a point singularity.

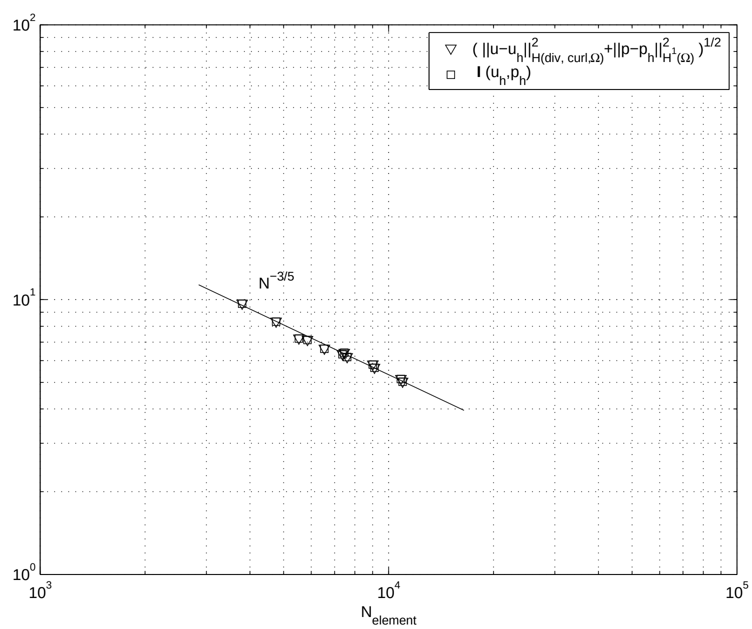

Figure 6: Error for DLSFEM in the point singularity problem. Triangles denote the error measured in the $H^1(\Omega) \times H(\mathrm{div}, \mathrm{curl}; \Omega)$-norm and squares denote the least-squares residual.

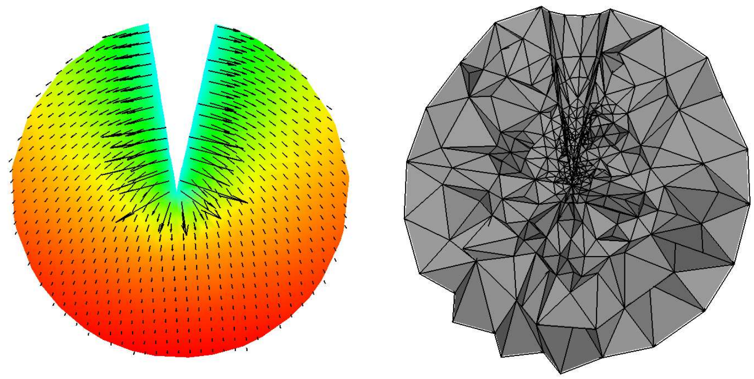

(a) *Solution* (b) *Refined mesh*

Figure 7: The solution and the refined mesh for the point singularity problem.

where H is the magnetic field intensity, B is the magnetic flux density, and J the imposed current density. The two fields H and B are related through the constitutive relation

$$B = \mu H, \tag{5.7}$$

where $\mu = \mu_r \mu_0$ is the magnetic permeability with $\mu_0 = 4\pi \times 10^{-7}$ H/m and $\mu_r > 0$. At the interface between two materials, equations (5.6) imply the continuity conditions

$$[H] \times n = 0, \tag{5.8a}$$
$$[B] \cdot n = 0, \tag{5.8b}$$

stating that the tangential components of H are continuous, as well as the normal component of B. In view of equation (5.7), the normal component $H \cdot n$ and the tangential components $B \times n$ will thus be discontinuous across an interface of discontinuity of μ. At the boundary, we have either a prescribed field, a symmetry condition or a perfectly conducting wall, $B \cdot n = 0$.

5.2.1 Model problem

We have previously reported problems in applying LSFEM to magnetostatic problems with realistic data [5]. Applying the discontinuous least-squares method to system (5.6), we have however successfully solved a model problems of this kind. Never the less, the mesh refinement indicator does not seem to yield optimal convergence. The problem is axisymmetric in order to make two dimensional reference computations possible, and is also reported in [3] and [4].

The geometry of this problem is described in Figure 10(a). A three dimensional view can be seen in Figure 10(b). The model consists of an iron cylinder core encircled by a copper winding. The configuration is enclosed in air and surrounded by a box with perfectly magnetic surfaces. The winding is modeled as a homogeneous copper coil.

	DLSFEM	Reference
No of elements	348 373	-
No of nodes	59 970	-
W_{air} (J)	$8.322 \times 10^{-7}(0.08)$	9.089×10^{-7}
W_{cu} (J)	$3.434 \times 10^{-8}(0.05)$	3.614×10^{-8}
W_{fe} (J)	$5.358 \times 10^{-10}(0.13)$	4.731×10^{-10}

Table 1: The computed magnetic energies compared with reference values using DLSFEM; the relative error is given in parenthesis. The reference values are from two dimensional computations done at ABB [4].

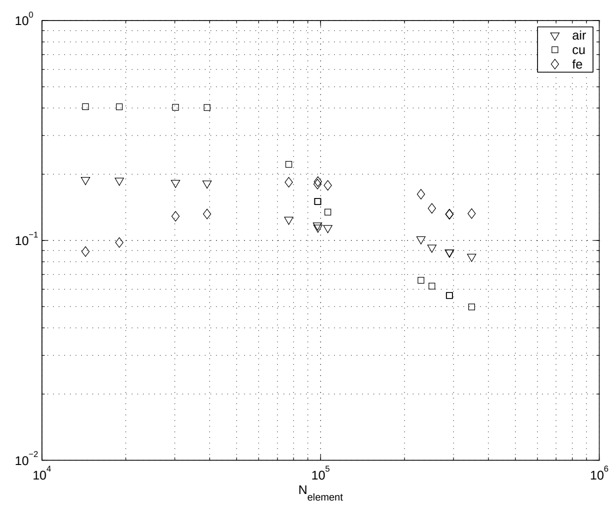

Figure 8: Relative error in the energy for DLSFEM in the magnetostatic problem. Triangles denote the error in the air region, squares represent the copper region, and diamonds the iron core.

Data for this problem are relative magnetic permeabilities $\mu_{r,Fe} = 10^4$ and $\mu_{r,Cu} = \mu_{r,air} = 1$, and the current density J is constant over the cross section of the coil with a total current of 1 A.

Reference computations in two dimensions done by ABB and reported in [4], gave the values of the magnetic energies in the different materials as listed in Table 1, where the magnetic energy is defined by

$$W_{\Omega^i} = \frac{1}{2} \int_{\Omega^i} B \cdot H \, dx. \tag{5.9}$$

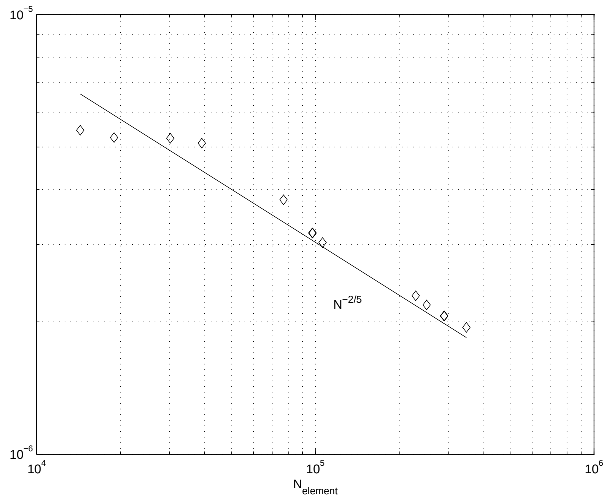

Figure 9: The least-squares residual for the magnetostatic example.

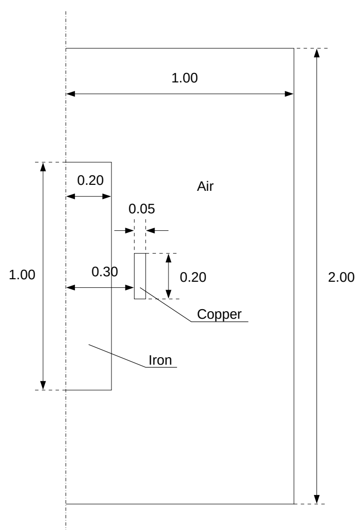

(a) *Geometry of the magnetostatic example*

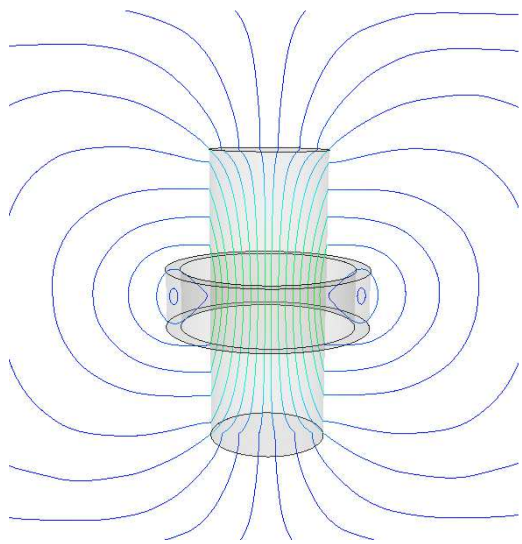

(b) *Field lines of the solution*

Figure 10: Geometry and the solution for the magnetostatic example.

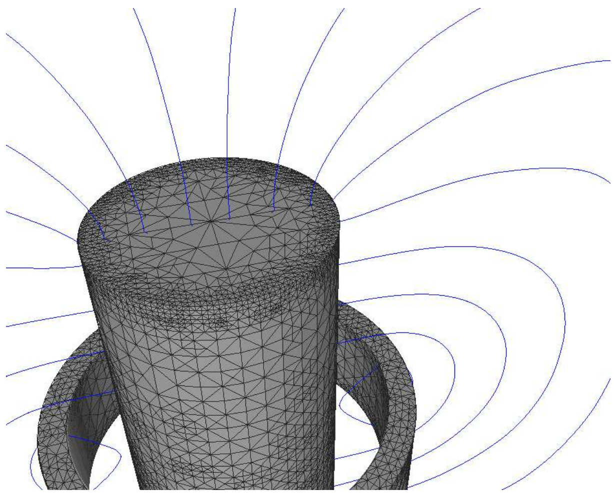

Figure 11: Detail of the mesh.

References

[1] C. Amrouche, C. Bernardi, M. Dauge, and V. Girault. Vector potentials in three-dimensional nonsmooth domains. *Math. Methods Appl. Sci.*, 21:823–864, 1998.

[2] T. Apel, S. Nicaise, and J. Schöberl. Crouzeix-Raviart type finite elements on anisotropic meshes. *Numer. Math.*, 89(2):193–223, 2001.

[3] R. Bergström. Least-squares finite element method with applications in electromagnetics. Preprint 10, Chalmers Finite Element Center, Chalmers University of Technology, 2002.

[4] R. Bergström, A. Bondeson, C. Johnson, M.G. Larson, Y. Liu, and K. Samuelsson. Adaptive finite element methods in electromagnetics. Technical Report 2, Swedish Institute of Applied Mathematics (ITM), 1999.

[5] R. Bergström and M.G. Larson. Discontinuous/continuous least-squares finite element methods for elliptic problems. Preprint 11, Chalmers Finite Element Center, Chalmers University of Technology, 2002. To appear in Math. Models Methods Appl. Sci.

[6] R. Bergström, M.G. Larson, and K. Samuelsson. The $\mathcal{L}\mathcal{L}^*$ finite element method and multigrid for the magnetostatic problem. Preprint 2, Chalmers Finite Element Center, Chalmers University of Technology, 2001.

[7] P.B. Bochev and M.D. Gunzburger. Finite element methods of least-squares type. *SIAM Rev.*, 40(4):789–837, 1998.

[8] A.-S. Bonnet-Ben Dhia, C. Hazard, and S. Lohrengel. A singular field method for the solution of Maxwell's equations in polyhedral domains. *SIAM J. Appl. Math.*, 59(6):2028–2044, 1999.

[9] J.H. Bramble, R.D. Lazarov, and J.E. Pasciak. A least-squares approach based on a discrete minus one inner product for first order systems. *Math. Comp.*, 66(219):935–955, 1997.

[10] Z. Cai, T.A. Manteuffel, and S.F. McCormick. First-order system least squares for second-order partial differential equations. II. *SIAM J. Numer. Anal.*, 34(2):425–454, 1997.

[11] Y. Cao and M.D. Gunzberger. Least-squares finite element approximations to solutions of interface problems. *SIAM J. Numer. Anal.*, 35(1):393–405, 1998.

[12] Z.M. Chen, Q. Du, and J. Zou. Finite element methods with matching and nonmatching meshes for Maxwell equations with discontinuous coefficients. *SIAM J. Numer. Anal.*, 37:1542–1570, 2000.

[13] C.L. Cox and G.J. Fix. On the accuaracy of least squares methods in the presence of corner singularities. *Comp. & Maths. with Appls.*, 10(6):463–475, 1984.

[14] L. Formaggia and S. Perotto. New anisotropic a priori estimates. *Numer. Math.*, 89:641–667, 2001.

[15] V. Girault and P.A. Raviart. *Finite Element Methods for Navier-Stokes Equations.* Springer-Verlag, 1986.

[16] P. Grisvard. *Elliptic Problems in Nonsmooth Domains.* Pitman Publishing Inc., 1985.

[17] J.D. Jackson. *Classical Electrodynamics.* John Wiley & Sons, 2nd edition, 1975.

[18] J.-L. Liu. Exact a posteriori error analysis of the least-squares finite element method. *Appl. Math. Comput.*, 116:297–305, 2000.

[19] T.A. Manteuffel, S.F. McCormick, and G. Starke. First-order system of least-squares for second order elliptic problems with discontinuous coefficients. To appear.

[20] J.E. Pasciak and J. Zhao. Overlapping schwarz methods in h(curl) on nonconvex domains.

[21] A.I. Pehlivanov, G.F. Carey, and P.S. Vassilevski. Least-squares mixed finite element methods for non-selfadjoint problems: I. error estimates. *Numer. Math.*, 72:501–522, 1996.

[22] L.R. Scott and S. Zhang. Finite element interpolation of nonsmooth functions satisfying bundary conditions. *Math. Comp.*, 54:483–493, 1990.

[23] K.G. Siebert. An a posteriori error estimator for anisotropic refinement. *Numer. Math.*, 73(3):373–398, 1996.

Chalmers Finite Element Center Preprints

2001–01 *A simple nonconforming bilinear element for the elasticity problem*
Peter Hansbo and Mats G. Larson

2001–02 *The $\mathcal{LL}^*$ finite element method and multigrid for the magnetostatic problem*
Rickard Bergström, Mats G. Larson, and Klas Samuelsson

2001–03 *The Fokker-Planck operator as an asymptotic limit in anisotropic media*
Mohammad Asadzadeh

2001–04 *A posteriori error estimation of functionals in elliptic problems: experiments*
Mats G. Larson and A. Jonas Niklasson

2001–05 *A note on energy conservation for Hamiltonian systems using continuous time finite elements*
Peter Hansbo

2001–06 *Stationary level set method for modelling sharp interfaces in groundwater flow*
Nahidh Sharif and Nils-Erik Wiberg

2001–07 *Integration methods for the calculation of the magnetostatic field due to coils*
Marzia Fontana

2001–08 *Adaptive finite element computation of 3D magnetostatic problems in potential formulation*
Marzia Fontana

2001–09 *Multi-adaptive galerkin methods for ODEs I: theory & algorithms*
Anders Logg

2001–10 *Multi-adaptive galerkin methods for ODEs II: applications*
Anders Logg

2001–11 *Energy norm a posteriori error estimation for discontinuous Galerkin methods*
Roland Becker, Peter Hansbo, and Mats G. Larson

2001–12 *Analysis of a family of discontinuous Galerkin methods for elliptic problems: the one dimensional case*
Mats G. Larson and A. Jonas Niklasson

2001–13 *Analysis of a nonsymmetric discontinuous Galerkin method for elliptic problems: stability and energy error estimates*
Mats G. Larson and A. Jonas Niklasson

2001–14 *A hybrid method for the wave equation*
Larisa Beilina, Klas Samuelsson and Krister Åhlander

2001–15 *A finite element method for domain decomposition with non-matching grids*
Roland Becker, Peter Hansbo and Rolf Stenberg

2001–16 *Application of stable FEM-FDTD hybrid to scattering problems*
Thomas Rylander and Anders Bondeson

2001–17 *Eddy current computations using adaptive grids and edge elements*
Y. Q. Liu, A. Bondeson, R. Bergström, C. Johnson, M. G. Larson, and K. Samuelsson

2001–18 *Adaptive finite element methods for incompressible fluid flow*
Johan Hoffman and Claes Johnson

2001–19 *Dynamic subgrid modeling for time dependent convection–diffusion–reaction equations with fractal solutions*
Johan Hoffman

2001–20 *Topics in adaptive computational methods for differential equations*
Claes Johnson, Johan Hoffman and Anders Logg

2001–21 *An unfitted finite element method for elliptic interface problems*
Anita Hansbo and Peter Hansbo

2001–22 *A P^2–continuous, P^1–discontinuous finite element method for the Mindlin-Reissner plate model*
Peter Hansbo and Mats G. Larson

2002–01 *Approximation of time derivatives for parabolic equations in Banach space: constant time steps*
Yubin Yan

2002–02 *Approximation of time derivatives for parabolic equations in Banach space: variable time steps*
Yubin Yan

2002–03 *Stability of explicit-implicit hybrid time-stepping schemes for Maxwell's equations*
Thomas Rylander and Anders Bondeson

2002–04 *A computational study of transition to turbulence in shear flow*
Johan Hoffman and Claes Johnson

2002–05 *Adaptive hybrid FEM/FDM methods for inverse scattering problems*
Larisa Beilina

2002–06 *DOLFIN - Dynamic Object oriented Library for FINite element computation*
Johan Hoffman and Anders Logg

2002–07 *Explicit time-stepping for stiff ODEs*
Kenneth Eriksson, Claes Johnson and Anders Logg

2002–08 *Adaptive finite element methods for turbulent flow*
Johan Hoffman

2002–09 *Adaptive multiscale computational modeling of complex incompressible fluid flow*
Johan Hoffman and Claes Johnson

2002–10 *Least-squares finite element method with applications in electromagnetics*
Rickard Bergström

2002–11 *Discontinuous/continuous least-squares finite element methods for Elliptic Problems*
Rickard Bergström and Mats G. Larson

2002–12 *Discontinuous least-squares finite element methods for the Div-Curl problem*
Rickard Bergström and Mats G. Larson

These preprints can be obtained from

`www.phi.chalmers.se/preprints`